Excited States of Free Base Phthalocyanine Studied by the SAC-CI Method

Kazuo Toyota,[†] Jun-ya Hasegawa,[†] and Hiroshi Nakatsuji*[,†,‡]

Department of Synthetic Chemistry and Biological Chemistry, Faculty of Engineering, Kyoto University, Sakyo-ku, Kyoto, 606-01, Japan, and Institute for Fundamental Chemistry, 34-4 Takano Nishi-Hiraki-cho, Sakyo-ku, Kyoto, 606, Japan

Received: June 14, 1996; In Final Form: September 30, 1996[⊗]

The SAC (symmetry adapted cluster)/SAC-CI method was used to calculate the ground and excited states of free base phthalocyanine (FBPc). This is the first accurate *ab initio* study of the excited states of FBPc. The calculated electronic spectrum agrees reasonably well with experimental results with regard to both energy and intensity. The relationships among the molecular structure, excitation energy, and spectral intensity are discussed, and the present results are compared with those for free base porphine (FBP) and free base tetrazaporphine (FBTAP) studied previously. Two important effects of skeletal changes are clarified; meso-tetraaza substitution and tetrabenzo substitution cause a large splitting between the HOMO and next HOMO levels and lead to a breakdown of the quasi-degeneracy of the two main configurations of the Q band, resulting in strong visible absorption due to the incomplete cancellation of the individual contributions to the transition dipole moment. This explains why Pc's are so useful as pigments. Further, a new assignment of the B (Soret) band is proposed. The broad experimental B band is composed of at least four states. The main peak of the B band is due to transitions from the orbital lower than the so-called "four orbitals", and the transitions arising from the "four orbitals" constitute the shoulder in the lower energy side of the band.

Introduction

Tens of thousands of tons of phthalocyanines (Pc's) are produced per year worldwide, and these are used mostly as commercial pigments due to their high thermal and chemical stability and intense color. Free base phthalocyanine (FBPc, $C_{32}N_8H_{18}$) is sometimes called tetrabenzotetraazaporphyrin. It differs from biologically important porphyrins such as chlorophyll in that it has an extended π-system characterized by four benzene rings, and the four meso positions are substituted by nitrogens. Tetraaza-substituted compounds without benzene rings, tetrazaporphines (TAP's), have also been synthesized[1] but are not of industrial importance. The electronic structures of Pc's are particularly interesting because Pc's are not only pigments but also promising candidates for use in electrochromic devices,[2,3] photovoltaic cells,[4] electrophotography,[5] photochemical hole burning,[6] conductive material,[7] etc.

Gouterman et al. proposed a "four-orbital model" [8] to describe the lower excitation peaks of porphyrins, the Q band in visible region and the B (or Soret) band in the UV region, based on Parriser−Parr−Pople calculations. Gouterman also studied azaporphins and roughly succeeded in explaining the effect of tetraaza substitution within this model.[9] Lee et al. studied the excited states of dianions of porphine, TAP, and Pc using a semiempirical CNDO-CI calculation.[10] Orti and Brédas calculated some excited states of FBPc by the valence effective Hamiltonian (VEH) method, and the resulting excitation energies of the visible Q band were in good agreement with experimental findings.[11] However, the use of scaling and level-shift constants for the orbital energies in their calculations may be problematic. Some *ab initio* studies of FBPc have recently appeared. Ghosh et al. calculated the ground states of FBPc, FBTAP, and their derivatives by the direct SCF method and discussed substitution effects in Pc and TAP macrocycles.[12,13]

In this study, we examined the ground and excited states of FBPc using the SAC (symmetry adapted cluster)[14] and SAC-CI[15−17] methods.[18,19] Recently, the SAC/SAC-CI method has been applied to several porphyrins, such as free base porphine (FBP),[20] magnesium porphine (MgP),[21] free base tetrazaporphine (FBTAP),[22] oxyheme,[23] and carboxyheme,[24] and has reproduced their absorption spectra in good agreement with experimental results. Pc's have intense absorption bands in the visible region, which makes them useful as pigments. We study here the relationship between the molecular structure and spectral intensities, especially in the visible (Q band) and near-UV (B band) regions. The effects of tetrabenzo and meso-tetraaza substitutions on the excited states of porphyrin macrocycles are discussed through comparisons with previous SAC-CI studies on FBP[20] and FBTAP.[22] We elucidate why the visible absorptions of Pc's are so strong and also characterize the nature of the B band. Traditionally, the B bands of porphyrins are assigned to the counterpart states of the Q bands based on the "four-orbital model",[8] but we show that a different assignment is more suitable for the so-called B band of FBPc.

Calculations

The neutron diffraction experimental geometry of Hoskins et al.[25] was determined after idealization of the skeleton to D_{4h} symmetry. They concluded that the inner hydrogens appear to be "four half hydrogens" associated with the four nitrogens of the pyrroles. However, we adopt the "bonded model", i.e., the inner hydrogens are localized on a diagonally opposed pair of nitrogens, which is true in the case of FBP,[26] since we aim to reveal the effect of the step-by-step variation of the skeleton from FBP, via FBTAP, to FBPc. The FBPc plane is put on the *xy* plane, and the N−H bond is on the *x* axis, as shown in Figure 1.

The Gaussian basis set is of double-ζ quality for the valence 2p orbitals. We used the Huzinaga (63/5)/[2s2p] set[27] for carbon and nitrogen and the (4)/[1s] set[28] for hydrogen. The total number of contracted GTOs is 338. The Hartree−Fock SCF

* To whom correspondence should be addressed.
† Kyoto University.
‡ Institute for Fundamental Chemistry.
⊗ Abstract published in *Advance ACS Abstracts,* December 15, 1996.

S1089-5639(96)01763-X CCC: $14.00

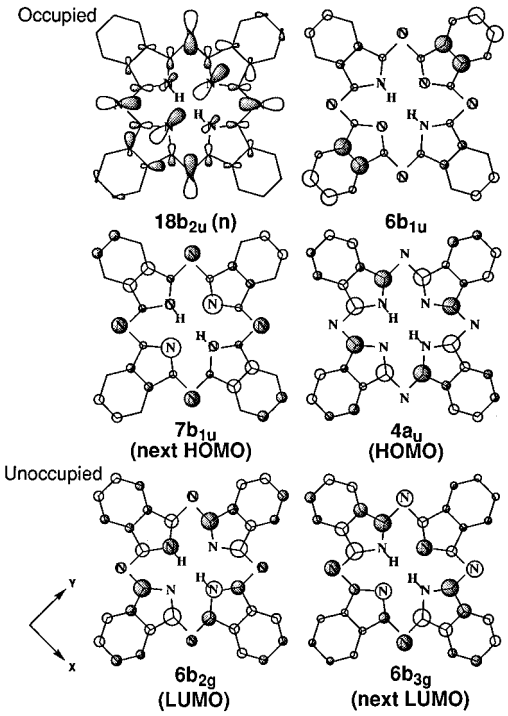

Figure 1. Occupied ($18b_{2u}$, $6b_{1u}$, $7b_{1u}$, and $4a_u$) and unoccupied ($6b_{3g}$ and $6b_{2g}$) MOs, which have a π character except for the $18b_{2u}$ MO.

TABLE 1: Dimensions of the SAC/SAC-CI Calculations of FBPc

symmetry	after selection	before selection	threshold ($\pi-\pi^*$)
ground state: SAC			
^1A_g	13 717	23 960 107	2×10^{-5} (1×10^{-5})
excited state: SAC-CI			
$^1B_{1u}$	49 277	21 488 562	1×10^{-6} (5×10^{-7})
$^1B_{2u}$	95 450	23 950 559	1×10^{-6} (5×10^{-7})
$^1B_{3u}$	86 710	23 950 466	1×10^{-6} (5×10^{-7})

orbitals, calculated using the HONDO program,[29] consist of 133 occupied and 205 unoccupied MOs.

In the SAC/SAC-CI calculations, only the 1s core orbitals of carbon and nitrogen are frozen; the higher 93 occupied MOs and all 205 unoccupied MOs are included in the active space. The total number of active orbitals is as high as 298. All of the single and selected double excitations within this active space are included in the linked term.[18,30] The selection scheme in the SAC-CI calculation is modified slightly[20] from the original[30] by adding the SE-CI coefficients of the reference configuration to the second-order perturbation energy expression to reflect the weight of the reference configuration in the selection scheme. The numbers of the linked configurations[18,30] are summarized in Table 1. For the ground state, energy thresholds of 1×10^{-5} and 2×10^{-5} hartree are used for the $\pi-\pi^*$ and other excitations, respectively. For the singlet excited states, the energy thresholds are 5×10^{-7} for $\pi-\pi^*$ and 1×10^{-6} for the other excitations. Single excitation configurations with SE-CI coefficients larger than 5×10^{-2} are used as reference configurations in the selection scheme. We only calculated the excited states of symmetries with nonzero oscillator strength. All calculations were carried out using a IBM RS6000/39H workstation with 128 MB of memory.

Ground State and Orbital Energy Levels

The energies and the natures of the HF MOs in the HOMO−LUMO region are shown in Table 2, and sketches of the four orbitals in the HOMO−LUMO region and the two lower MOs,

TABLE 2: HF Orbital Energies and Characters of FBPc

symmetry	character	orbital energy (eV)
	Higher Occupied Orbitals	
$20a_g$	n(meso N)	−13.063
$17b_{2u}$	n(meso N)	−12.959
$3b_{2g}$	π	−12.517
$18b_{3u}$	n(meso N)	−12.089
$21a_g$	n(pyrrole N)	−11.981
$3b_{3g}$	π	−11.938
$18b_{2u}$	n(pyrrole N)	−11.674
$15b_{1g}$	n(meso N)	−11.594
$2a_u$	π(benzene)	−10.372
$5b_{1u}$	π	−10.229
$4b_{2g}$	π(benzene)	−9.930
$4b_{3g}$	π(benzene)	−9.708
$3a_u$	π(benzene)	−9.649
$5b_{2g}$	π(benzene)	−9.490
$6b_{1u}$	π(benzene)	−9.167
$5b_{3g}$	π(benzene)	−9.071
$7b_{1u}$	π	−8.923
$4a_u$	π	−5.777
	Lower Unoccupied Orbitals	
$6b_{2g}$	π	−0.708
$6b_{3g}$	π	−0.492
$5a_u$	π(benzene)	2.135
$8b_{1u}$	π(benzene)	2.362
$7b_{2g}$	π(benzene)	2.694
$9b_{1u}$	π(benzene)	3.004
$7b_{3g}$	π(benzene)	3.039
$6a_u$	π(benzene)	4.253
$8b_{3g}$	π(benzene)	4.285
$8b_{2g}$	π(benzene)	4.431

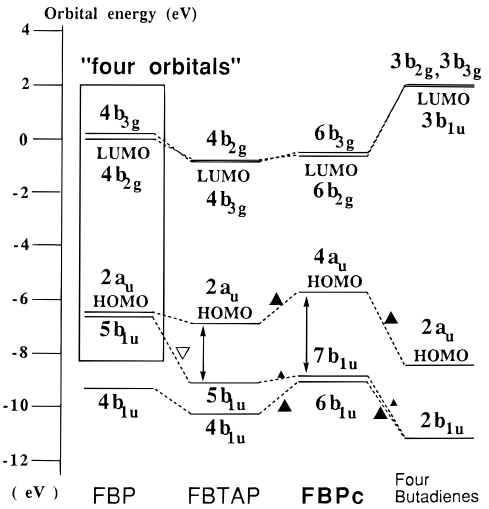

Figure 2. Orbital energies of the "four orbitals" and the lower b_{1u} MO of FBP, FBTAP, and FBPc. The meso-tetraaza substitution lowers the energy of the next HOMO (unfilled triangle), and the tetrabenzo substitution raises the energy of the HOMO (larger filled triangle).

which are pertinent to the following discussions, are shown in Figure 1. The energy levels of the MOs related to the lower excitations are illustrated in Figure 2 for FBP, FBTAP, and FBPc. Six lone-pair orbitals on nitrogens gather in the energy region from −13.1 to −11.6 eV. The pyrrole N lone pairs predominate in the $21a_g$ and $18b_{2u}$ MOs, and the meso N lone pairs predominate in the $20a_g$, $17b_{2u}$, $18b_{3u}$, and $15b_{1g}$ MOs. The $18b_{2u}$ MO, which gives the lowest $n-\pi^*$ excitation, is illustrated in Figure 1.

The π-type orbitals gather in the HOMO−LUMO region. The HOMO is $4a_u$ with nodes on the meso nitrogens. This is consistent with a previous VEH calculation[11] and *ab initio* calculations.[12,13] As shown in Figure 2, the HOMO energy of FBPc is higher than that of FBP and FBTAP, which is consistent with the experimental first IPs for FBP[31] (6.9 eV) and FBPc[32]

TABLE 3: SAC-CI Results for FBPc Compared with Experimental Findings

SAC-CI						experimental
state	main configuration ($\|C\| \geq 0.30$)	nature[a]	excitation energy (eV)	oscillator strength	polarization	excitation energy (eV)
$1B_{3u}$	$+0.87(4a_u \rightarrow 6b_{3g}) + 0.35(7b_{1u} \rightarrow 6b_{2g})$	$\pi \rightarrow \pi^*$	1.30	1.050	*x*	1.81 (Q_x)
$1B_{2u}$	$+0.92(4a_u \rightarrow 6b_{2g})$	$\pi \rightarrow \pi^*$	1.51	0.585	*y*	1.99 (Q_y)
$2B_{3u}$	$+0.76(7_{b1u} \rightarrow 6b_{2g}) + 0.44(6b_{1u} \rightarrow 6b_{2g})$	$\pi \rightarrow \pi^*$	3.10	0.589	*x*	3.2 (B tail)
$2B_{2u}$	$-0.87(7_{b1u} \rightarrow 6b_{3g})$	$\pi \rightarrow \pi^*$	3.55	0.554	*y*	3.5 (B shoulder)
$3B_{3u}$	$-0.81(6b_{1u} \rightarrow 6b_{2g}) + 0.36(7b_{1u} \rightarrow 6b_{2g})$	π(b) $\rightarrow \pi^*$	3.96	1.792	*x*	3.65 (B main peak)
$1B_{1u}$	$-0.93(18b_{2u} \rightarrow 6b_{3g})$	n(p) $\rightarrow \pi^*$	3.96	0.012	*z*	
$3B_{2u}$	$+0.86(6b_{1u} \rightarrow 6b_{3g})$	π(b) $\rightarrow \pi^*$	4.07	1.246	*y*	3.9 (B main peak)
$2B_{1u}$	$+0.92(18b_{3u} \rightarrow 6b_{2g})$	n(m) $\rightarrow \pi^*$	4.31	0.004	z	
$4B_{2u}$	$+0.91(4a_u \rightarrow 7b_{2g})$	$\pi \rightarrow \pi$(b)*	4.32	0.139	*y*	4.1 (B shoulder)
$5B_{2u}$	$+0.84(3a_u \rightarrow 6b_{2g})$	π(b) $\rightarrow \pi^*$	4.51	0.012	*y*	
$4B_{3u}$	$+0.86(4a_u \rightarrow 7b_{3g})$	$\pi \rightarrow \pi$(b)*	4.58	0.009	*x*	
$5B_{3u}$	$+0.52(3a_u \rightarrow 6b_{3g}) - 0.50(5b_{1u} \rightarrow 6b_{2g}) + 0.38(4a_u \rightarrow 7b_{3g})$	π(b) $\rightarrow \pi^*$	4.81	0.003	*x*	

[a] n(p) and n(m) denote lone-pair orbitals which have large amplitudes on the pyrrole and meso nitrogens, respectively, and π(b) denotes π-type orbitals which have a large amplitude on the benzenoid carbons.

(6.4 eV). This destabilization of the HOMO can be explained by the concept of orbital interaction. The MOs of FBPc in this region are formed by interaction between the two π-systems of the FBTAP skeleton and the 16 residual carbons regarded as four *cis*-1,3-butadienes (referred to as "4B"). Since the HOMO of FBTAP (at −6.98 eV) and that of 4B (at −8.54 eV) are relatively close in energy and have the same a_u symmetry, the antibonding MO they comprise, the HOMO of FBPc, is considerably destabilized.

In a previous study of FBTAP, we found a lowering of the next HOMO by meso-tetraaza substitution and elucidated its effect on the lower excited states.[22] The next HOMO of FBPc is $7b_{1u}$ at −8.92 eV, which is shifted down as in FBTAP. In contrast to the HOMO, the next HOMO energy is rather free from the influence of the tetrabenzo substitution. The $2b_{1u}$ MO of 4B (at −12.3 eV), which is the highest occupied MO with this symmetry, is much lower than the next HOMO of FBTAP (at −9.15 eV). Therefore, the orbital interaction between the central and peripheral π-systems is weaker in the next HOMO than in the HOMO. The $2b_{1u}$ MO of 4B is closer to the lower $4b_{1u}$ MO of FBTAP (at −10.30 eV) rather than to the next HOMO, and the "antibonding" $6b_{1u}$ MO of FBPc is shifted considerably up. Thus, the energy difference between the HOMO and the next HOMO of FBPc increases to 3.15 eV, while in FBP this energy difference is as small as 0.17 eV.[20]

The LUMO and the next LUMO of FBTAP are $4b_{2g}$ and $4b_{3g}$ and are at −0.891 and −0.847 eV, respectively. The lowest unoccupied MOs with these symmetries of 4B are in such a higher energy region (at +1.97 eV) that the influence of the tetrabenzo substitution is small for the LUMO and the next LUMO of FBPc. Consequently, the HOMO−LUMO gap decreases.

For FBP, FBTAP, and FBPc, the variations in the excitation energies and the intensities of the visible and near−UV peaks can be explained by the orbital energy shifts shown above. In the next section, we discuss their effect on the excited states, especially the key role of the widening of the energy gap between the two quasi-degenerate HOMOs in the intensity and energy variations of the Q and B bands.

Excited States

Table 3 summarizes the excited states of FBPc calculated by the SAC-CI method. It shows the optically allowed ten $\pi-\pi^*$ and two $n-\pi^*$ excited states.

The electronic spectra of FBPc are shown in Figure 3. The upper panel is the experimental spectrum,[33] and the lower panel is the SAC-CI theoretical spectrum. The most important feature

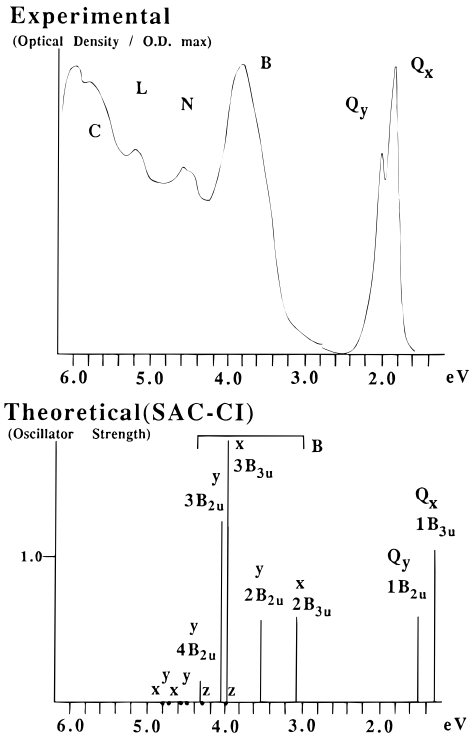

Figure 3. Electronic excitation spectra of FBPc observed in the vapor phase[33] and calculated by the SAC-CI method. The optically allowed weak transition is indicated by a filled circle.

of the FBPc spectrum is that the visible Q bands have much greater intensities than those of FBP. The observed intensity ratio of the Q_x band/B band is 0.02 for FBP in benzene[34] and 2.9 for FBPc in 1-chloronaphthalene.[35]

Q Band. The Q band in the experimental spectrum is composed of the two strong peaks Q_x and Q_y at 1.81 and 1.99 eV, respectively, and Q_x is more intense than Q_y. Based on SAC-CI calculations, Q_x and Q_y are assigned to the $1B_{3u}$ and $1B_{2u}$ states calculated at 1.30 and 1.51 eV, respectively. No other allowed excited states are found in the energy region below 2.3 eV. The errors in the excitation energy are 0.51 and 0.48 eV, respectively, which are large but may not be so bad considering that many double-excitation operators were not included in the linked term, as shown in Table 1, to simplify the computations. The calculated oscillator strengths of the Q_x and Q_y bands are 1.050 and 0.585, respectively, which are quite large in comparison with those of FBP, 1.13×10^{-3} and 5.66×10^{-3}, respectively, which agrees with the experimental results. The intensity ratio of Q_x/Q_y is also well-reproduced; Q_x is larger

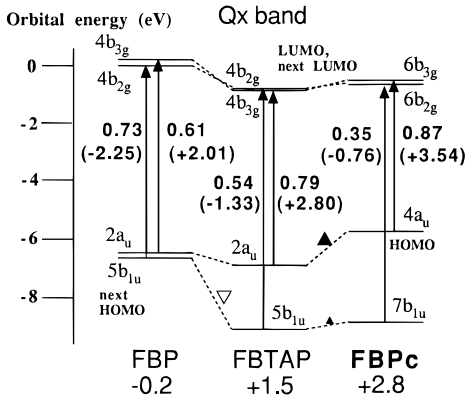

Figure 4. Incomplete cancellations of the transition dipole moments in the Q_x band due to the unbalanced superposition of the transitions in FBTAP and FBPc in contrast to FBP. The SAC-CI coefficients and the contributions to the transition moments (in parentheses) are given. The net moments are also shown at the bottom of the figure.

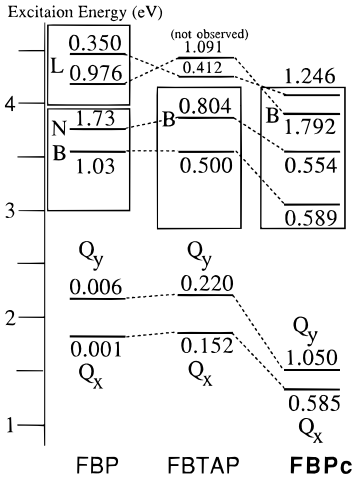

Figure 5. Comparison of the excitation energies and the oscillator strengths of the excited states of FBP, FBTAP, and FBPc calculated by the SAC-CI method. States with the same nature are connected by a dotted line. The rectangles indicate the range of the broad band in the experimental spectra.

than Q_y, in contrast to the case of FBP. The $1B_{3u}$ and $1B_{2u}$ states are polarized in the *x* and *y* directions, respectively. (The *x* axis is along the N−H H−N bonds.) The theoretical prediction that the Q_x band is polarized perpendicularly to the Q_y is in agreement with experimental findings.[36] We follow the general convention that the lower energy Q band is Q_x and the upper band is Q_y, without implying any absolute orientation, although our theoretical ordering of the Q band polarization is the same as that observed experimentally and calculated by SAC-CI for FBP[20] and FBTAP.[22]

One of the most important properties of Pc's is that strong absorption bands exist in the visible region, which is why Pc's are used as pigments. The absorption spectrum of FBTAP also shows strong Q bands,[1,37] and we elucidated the origin of its strength in a previous study.[22] In FBPc, the same mechanism has an even greater effect than in FBTAP.

Figure 4 shows the coefficients of the main configurations and their contributions to the transition dipole moments of the Q_x bands of FBP, FBTAP, and FBPc. In these three compounds, the Q band is written as a superposition of two main configurations. For example, the $1B_{3u}$ state of FBPc which represents the Q_x band is written as a superposition of the two configurations $4a_u \rightarrow 6b_{3g}$ and $7b_{1u} \rightarrow 6b_{2g}$, as seen in Table 3. In FBP, the absolute values of the coefficients of the corresponding two main configurations are approximately equal in both the Q_x and Q_y states (e.g., 0.73 and 0.61 for Q_x), reflecting the quasi-degeneracy of the HOMO and the next HOMO. The contributions of the two main configurations to the transition dipole moment are of opposite signs (e.g., −2.25 and +2.01 for Q_x), and therefore, when the weights of the configurations are equal, the moment is canceled out, which explains why the Q band of FBP is weak.[38] On the other hand, in FBTAP and FBPc the coefficients of the two main configurations in the Q band are unbalanced, reflecting the orbital energy differences between the two excitations. For example, the Q_x band of FBPc consists of major $(0.87)(4a_u \rightarrow 6b_{3g})$ and minor $(0.35)(7b_{1u} \rightarrow 6b_{2g})$ configurations because the energy difference between $4a_u$ and $6b_{3g}$ is smaller than that between $7b_{1u}$ and $6b_{2g}$. This unbalanced superposition of the configurations results in a large transition moment, as shown at the bottom of Figure 4.

For FBTAP, we previously concluded[22] that the strong intensities of the Q bands in the visible region are due to the breakdown of the quasi-degeneracy of the two main configurations due to lowering of the next HOMO, which is localized on the meso nitrogens. Furthermore, in FBPc, extension of the conjugated π-system destabilizes the HOMO much more than the next HOMO, so that the breakdown of the quasi-degeneracy increases and the predominance of the transition from the HOMO increases in the Q band. Therefore, the energy shifts of the next HOMO and HOMO by meso-tetraaza and tetrabenzo substitutions result in an extremely intense Q band in Pc's.

The excitation energies and oscillator strengths for FBP,[20] FBTAP,[22] and FBPc calculated by the SAC-CI method are compared in Figure 5. Since the HOMO−LUMO gap of FBPc is narrower than that of FBTAP (see Figure 2), the Q band of FBPc shows a bathochromic shift, consistent with experimental findings.

B Band. The B band of FBPc is quite strong and broad. These features increase in the order FBP, FBTAP, and FBPc. The present SAC-CI study revealed that at least six allowed transitions exist in this area. The $2B_{3u}$, $2B_{2u}$, $3B_{3u}$, $1B_{1u}$, $3B_{2u}$, and $2B_{1u}$ states are calculated at 3.10, 3.55, 3.96, 3.96, 4.07, and 4.31 eV, respectively. The oscillator strengths of the $2B_{3u}$ and $2B_{2u}$ states are calculated to be 0.589 and 0.554, respectively. These correspond to the tail at around 3.2 eV and the shoulder at around 3.5 eV on the right-hand side of the main peak (see Figure 3). The B band main peak is assigned to the $3B_{3u}$ and $3B_{2u}$ states, whose calculated oscillator strengths of 1.792 and 1.246, respectively, are larger than those of any other transitions calculated here.

We note that the third pair ($3B_{3u}$ and $3B_{2u}$) of the allowed $\pi-\pi^*$ states is assigned to the main peak. The second pair ($2B_{3u}$ and $2B_{2u}$) may be approximated by the "four-orbital model", but the third pair is not described by the "four-orbital model". The B bands of other porphyrins, such as FBP,[20] MgP,[21] and FBTAP,[22] were assigned to the $2B_{3u}$ and/or $2B_{2u}$ states whose main configurations arise from the traditional "four-orbital model". The $3B_{3u}$ and $3B_{2u}$ states of FBP were assigned to the relatively weak L band in the energy region higher than the B band.[20] This difference arises from the bathochromic shift of the $3B_{3u}$ and $3B_{2u}$ states and the increase in their oscillator strengths (see Figure 5). These states are mainly written as the transition from the $6b_{1u}$ MO, which can be regarded as the HOMO of the four benzene rings shown in Figure 1, to the LUMO or the next LUMO. The $6b_{1u}$ MO is lower than the "four orbitals" but is considerably destabilized by antibonding interaction, as we have already pointed out, so that it is close to the next HOMO. This shift of the $6b_{1u}$ MO causes a decrease in the transition energy.

The $6b_{1u}$ MO of FBPc resembles the $4b_{1u}$ MO of FBP except for a large amplitude on the peripheral 16 carbons. This large

amplitude on the periphery of the molecule causes an increase in the transition dipole moments. In FBPc, the transition dipole moment of the excitation $6b_{1u} \rightarrow 6b_{2g}$ (LUMO), which is the main configuration of the $3B_{3u}$ state, is as large as 1.76, while in FBP that of the excitation $4b_{1u} \rightarrow 4b_{2g}$(LUMO) is 0.73. Thus, the oscillator strengths of the $3B_{3u}$ and $3B_{2u}$ states are larger in FBPc than in FBP. Comparing the experimental electronic spectra of thin-film unsubstituted and chlorinated FBPc,[39] the B band is more influenced by chlorination on the benzene rings than the Q band. This indicates that the B band includes the transition related to the benzene rings, which supports our new assignment.

With regard to the color of the molecule, the bathochromic shift of the visible Q band as a reflection of the narrower HOMO−LUMO gap in FBPc than in FBP changes the color from violet-blue (FBTAP)[1] to bluish-green (FBPc). The concept of orbital interaction between the TAP skeleton and the 16 external carbons can be useful for understanding substitution effects on the color of Pc's. For example, when a substituent shifts the HOMO energy of 4B up, the antibonding interaction in the HOMO of the substituted Pc is expected to increase, and the Q bands shift to a lower energy region. Since the broad B band has some overlap with the higher energy edge of the visible region, a similar approach to the shifts of the next HOMO ($7b_{1u}$) and "the HOMO of benzene rings" ($6b_{1u}$) may account for changes in the color of Pc's. When these orbitals shift up or down, the B band is roughly expected to show a bathochromic or hypsochromic shift, respectively.

Other Transitions with Weak Intensities. The $1B_{1u}$ and $2B_{1u}$ states are the first and second allowed n−π* transitions, and are polarized in the out-of-plane *z* direction. These are weak transitions with calculated oscillator strengths of 0.012 and 0.004, respectively. The location of the first n−π* transition differs between FBP and azaporphyrins like FBTAP and FBPc: in FBP[20] it is a component of the L band at an energy region higher than the B band, while in FBPc and FBTAP[22] it shifts down into the B band region. The meso nitrogens play some role in this lowering of the lowest allowed n−π* transition. The existence of the n−π* transition in the B band region also accounts for the broadness of this band. Hochstrasser and Marzzacco observed the low-temperature electronic spectra of several aromatic azines and reported that band broadening was seen in the overlap of the n−π* and π−π* states.[40] They concluded that vibronic coupling between the n−π* and π−π* states is greater than those between π-π* states.

The $4B_{2u}$ excited states are calculated at 4.32 eV, and the calculated oscillator strength is 0.139, which is not small. We may interpret this state as representing the shoulder on the left-hand side of the B band. Another possibility is to assign it to the N band. However, it is difficult to assign this and higher observed peaks.

We calculated three other allowed transitions in the higher energy region. The $5B_{2u}$, $4B_{3u}$, and $5B_{3u}$ excited states are calculated at 4.51, 4.58, and 4.81 eV, respectively. However, since only very small oscillator strengths are calculated for these transitions (0.012, 0.009, and 0.003, respectively), these transitions would not be found experimentally.

Conclusion

SAC-CI calculations were performed to understand the electronic absorption spectrum of FBPc. The results may be summarized as follows.

(i) Breakdown of the quasi-degeneracy between the HOMO and next HOMO, which leads to an unbalanced superposition of the two main configurations of the Q bands, is caused by two structural factors: (1) the next HOMO is stabilized by meso-tetraaza substitution since it has large amplitudes on the meso nitrogens; (2) the HOMO is destabilized by a strong π antibonding interaction between the TAP skeleton and the four *cis*-butadienes (4B) since the HOMOs of these two parts have the same a_u symmetry and the energy difference between them is relatively small (within 1.6 eV). On the other hand, the next HOMO of the TAP skeleton has b_{1u} symmetry and is separated from the highest occupied b_{1u} orbital of 4B by about 3 eV, so that their orbital interaction is weak and the energy of the next HOMO is almost unchanged.

(ii) Breakdown of the quasi-degeneracy of the two main configurations causes an increase in the intensities of the Q_x and Q_y bands due to incomplete cancellation of the two contributions to the transition dipole moment. In FBTAP, only the first of the above factors is present, while both factors are present in Pc's. This explains why FBPc is strongly colored and Pc's are useful as commercial pigments.

(iii) The LUMO and the next LUMO energies are not influenced very much by meso nitrogen substitution and elongation of the conjugation. Therefore, the HOMO−LUMO gap is decreased, and the Q band shows a bathochromic shift to give a greenish color to Pc's.

(iv) The B band is composed of the $2B_{3u}$ and $2B_{2u}$ transitions and the $3B_{3u}$ and $3B_{2u}$ transitions. The former pair is weaker and corresponds to the tail and the shoulder on the low-energy side of the main peak, while the latter pair corresponds to the main strong peak. Therefore, the nature of the so-called "B band" of FBPc is different from those of other porphyrins, such as FBP, MgP, and FBTAP, whose B bands are assigned to the $2B_{3u}$ and/or $2B_{2u}$ states. This difference is due to the bathochromic shift of the $3B_{3u}$ and $3B_{2u}$ states and their increased intensities. These $3B_{3u}$ and $3B_{2u}$ states arise from the transitions from the $6b_{1u}$ MO, which has a large amplitude on the peripheral benzene carbons.

Acknowledgment. This study is dedicated to Prof. Saburo Nagakura, who has made such tremendous contributions to molecular spectroscopy and reactions in chemistry from both experimental and theoretical perspectives. This study was supported in part by a Grant-in-Aid for Scientific Research from the Ministry of Education, Science and Culture and by the New Energy and Industrial Technology Development Organization (NEDO).

References and Notes

(1) Linstead, R. P.; Whalley, M. *J. Chem. Soc.* **1952**, 4839.
(2) Riou, M.-T.; Auregan, M.; Clarisse, C. *J. Electroanal. Chem.* **1985**, *187*, 349.
(3) Sammells, A. F.; Pujare, N. U.; Clarisse, C. *J. Electrochem. Soc.* **1986**, *133*, 1065.
(4) Tang, C. W. *Appl. Phys. Lett.* **1986**, *48*, 183.
(5) Loutfy, R. O.; Hor, A. M.; Hsiao, C. K.; Baranyi, G.; Kazmaier, P. *Pure Appl. Chem.* **1988**, *60*, 1047.
(6) Rebane, L. A.; Gorokhovskii, A. A.; Kikas, J. V. *Appl. Phys.* **1982**, *B29*, 235.
(7) Marks, T. J. *Angew. Chem., Int. Ed. Engl.* **1990**, *29*, 857.
(8) Gouterman, M.; Wagnière, G. H.; Snyder, L. C. *J. Mol. Spectrosc.* **1963**, *11*, 108.
(9) Gouterman, M. *J. Chem. Phys.* **1959**, *30*, 1139.
(10) Lee, L. K.; Sabelli, N. H.; LeBreton, P. R. *J. Phys. Chem.* **1982**, *86*, 3926.
(11) Orti, E.; Brédas, J. L. *J. Chem. Phys.* **1988**, *89*, 1009.
(12) Ghosh, A.; Gassman, P. G.; Almlöf, J. *J. Am. Chem. Soc.* **1994**, *116*, 1932.
(13) Ghosh, A.; Fitzgerald, J.; Gassman, P. G.; Almlöf, J. *Inorg. Chem.* **1994**, *33*, 6057.
(14) Nakatsuji, H.; Hirao, K. *J. Chem. Phys.* **1978**, *68*, 2053.
(15) Nakatsuji, H. *Chem. Phys. Lett.* **1987**, *59*, 362.

(16) Nakatsuji, H. *Chem. Phys. Lett.* **1979**, *67*, 329.
(17) Nakatsuji, H. *Chem. Phys. Lett.* **1979**, *67*, 334.
(18) Nakatsuji, H. *Acta Chim. Hung.* **1992**, *129*, 719.
(19) Nakatsuji, H. *Chem. Phys.* **1983**, *75*, 425.
(20) Nakatsuji, H.; Hasegawa, J.; Hada, M. *J. Chem. Phys*. **1996**, *104*, 2321.
(21) Hasegawa, J.; Hada, M.; Nonoguchi, M.; Nakatsuji, H. *Chem. Phys. Lett.* **1996**, *250*, 159.
(22) Toyota, K.; Hasegawa, J.; Nakatsuji, H. *Chem. Phys. Lett.* **1996**, *250*, 437.
(23) Nakatsuji, H.; Hasegawa, J.; Ueda, H.; Hada, M. *Chem. Phys. Lett.* **1996**, *250*, 379.
(24) Nakatsuji, H.; Tokita, K.; Hasegawa, J.; Hada, M.; *Chem. Phys. Lett.* **1996**, *256*, 220.
(25) Hoskins, B. F.; Mason, S. A. *J. Chem. Soc., Chem. Commun*. **1969**, 554.
(26) Schaffer, A. M.; Gouterman, M. *Theor. Chim. Acta* **1972**, *25*, 62.
(27) Huzinaga, S.; Andzelm, J.; Krovkowski, M.; Radzio-Andzelm, E.; Sakai, Y.; Tatewaki, H. *Gaussian Basis Set for Molecular Calculations*; Elsevier: New York, 1984.
(28) Huzinaga, S. *J. Chem. Phys.* **1965**, *42*, 1293.
(29) Dupuis, M.; Maluendes, S. A. In *MOTECC*; Clementi, E., Ed.; ESCOM: Leiden, 1991; Chapter 12.
(30) Nakatsuji, H. *Chem. Phys*. **1983**, *75*, 425.
(31) Dupuis, P.; Roberge, R.; Sandorfy, C. *Chem. Phys. Lett.* **1980**, *75*, 434.
(32) Berkowitz, J. *J. Chem. Phys*. **1979**, *70*, 2819.
(33) Edwards, L.; Gouterman, M. *J. Mol. Spectrosc.* **1970**, *33*, 292.
(34) Eisner, U.; Linstead, R. P. *J. Chem. Soc*. **1955**, 3749.
(35) Whalley, M. *J. Chem. Soc*. **1961**, 866.
(36) Bondybey, V. E.; English, J. H. *J. Am. Chem. Soc.* **1979**, *101*, 3446.
(37) Dvornikov, S. S.; Knyukshto, V. N.; Kuzmitsky, V. A.; Shulga A. M.; Solovyov, K. N. *J. Lumin.* **1981**, *23*, 373.
(38) Weiss, C.; Kobayashi, H.; Gouterman, M. *J. Mol. Spectrosc.* **1965**, *16*, 415.
(39) Schechtman, B. H.; Spicer, W. E. *J. Mol. Spectrosc.* **1970**, *33*, 28.
(40) Hochstrasser, R. M.; Marzzacco, C. *J. Chem. Phys*. **1968**, *49*, 971.